



Bread baking using ohmic heating technology; a comprehensive study based on experiments and modelling



Timothée Gally, Olivier Rouaud*, Vanessa Jury, Alain Le-Bail

ONIRIS – GEPEA (UMR CNRS 6144), Site de la Géraudière CS 82225, 44322, Nantes Cedex 3, France

ARTICLE INFO

Article history:

Received 20 December 2015

Received in revised form

29 June 2016

Accepted 30 June 2016

Available online 2 July 2016

Keywords:

Ohmic heating

Baking

Dough

Modelling

Porosity

Electrical conductivity

ABSTRACT

Bread dough baking was investigated using ohmic heating technology. An experimental system was set up for the measurement of the electrical conductivity of bread dough during heating. The influence of temperature, salt content and degree of fermentation (porosity) on the electrical conductivity of dough was investigated. It was observed that it increased linearly with temperature, until starch gelatinisation during which the dough conductivity remained constant or slightly decreased. The conductivity increased linearly again after starch gelatinisation, but at a lower rate. The electrical conductivity of dough had a linear positive dependence on salt content, but decreased with increasing dough porosity. Numerical simulations of temperature increase were carried out and compared with experimental data. For a good correlation between numerical and experimental data, a corrective coefficient was numerically estimated and validated, taking into account mainly the conversion of electrical energy to heat, and geometric uncertainties. Numerical results showed that the linear evolution of temperature with heating time was mainly caused by heat losses.

© 2016 Elsevier Ltd. All rights reserved.

1. Introduction

Ohmic heating (OH), also known as Joule heating or resistive heating, is a heating process based on the passage of an electrical current through a material, which is used as an electrical resistance (Sastry, 1989). Its main advantages are rapid uniform heating, no residual heat transfer after shut-off of the current, and a high energy conversion efficiency (Sakr and Liu, 2014).

Food containing large amounts of water and ionic salts are the best candidates for OH (Sarang et al., 2008), and previous research has shown that most food contains ionic species, such as salts and acids (Palaniappan and Sastry, 1991).

Bread baking using OH was carried out for the first time by Baker (1939). The purpose of the apparatus that was developed (named an Electric Resistance Oven - ERO) was to bake dough with uniform heating. Using this apparatus, the authors studied starch gelatinisation, as well as the evolution of pressure and volume and gas formation in bread dough (Baker and Mize, 1939a, 1939b, 1941). They found that crustless bread could be produced. Later, bread baking using ERO technology came back to the fore. It was used to

study how shortenings and surfactants could improve loaf volume in bread (Junge and Hoseney, 1981), to evaluate the component interaction during heating and storage of baked products (Hoseney, 1986), to study cake baking and its viscosity (Shelke et al., 1990), to evaluate gas retention and bread firming (He and Hoseney, 1991a, 1991b; Martin et al., 1991), and to study the effect of pressure on bread crumb grain development (Hayman et al., 1998). More recently, OH was used by Luyts et al. (2013) to study the impact of moisture migration and amylopectin retrogradation on cake firming, and by Derde et al. (2014) to compare the moisture distribution between bread baked by ERO and by conventional heating. For each of these references, OH was used as a tool to produce bread with an isotropic heating in order to study specific characteristics. It was not considered a baking process as such.

During baking, swelling and gelatinisation of starch occur, which participate in the fixation of the structure (Martin et al., 1991). The detection of starch gelatinisation by OH has been studied by different authors. It was shown that when starch gelatinisation occurs, a noticeable change appears in the electrical conductivity of the sample. Li et al. (2004) and Wang and Sastry (1997) added sodium chloride to the starch suspensions in order to increase the electrical conductivities and observed that during starch gelatinisation, the rate of electrical conductivity increase slowed down. The reason proposed by the authors was that during

* Corresponding author.

E-mail address: olivier.rouaud@oniris-nantes.fr (O. Rouaud).

Nomenclature

a_e	constant of Eq. (10) ($S\ m^{-1}$)
a_S	constant of Eq. (11) ($S\ m^{-1}$)
A	electrode area (m^2)
b_e	constant of Eq. (10) ($S\ m^{-1}$)
b_S	constant of Eq. (11) ($S\ m^{-1}$)
C_p	heat capacity ($J.kg^{-1}.K^{-1}$)
E_r	average relative error (%)
ε	porosity (%)
I	current (A)
k	thermal conductivity ($W.m^{-1}.K^{-1}$)
L	gap between electrodes (m)
m	constant of Eq. (9) ($^{\circ}C^{-1}$)
m_d	mass of the dough sample (kg)

m_e	constant of Eq. (10) ($^{\circ}C^{-1}$)
m_i	mass of dough when weighing immersed in oil (kg)
m_S	constant of Eq. (11) ($^{\circ}C^{-1}$)
P	power (W)
Q_{GEN}	ohmic power source (W)
ρ_0	density of the degassed dough ($kg\ m^{-3}$)
ρ_{app}	apparent density of the dough ($kg\ m^{-3}$)
ρ_{oil}	density of the oil ($kg\ m^{-3}$)
R	resistance (Ω)
S	salt content (% dry basis)
σ	electrical conductivity ($S\ m^{-1}$)
σ_{25}	electrical conductivity at 25 $^{\circ}C$ ($S\ m^{-1}$)
V	voltage (V)
V_{cell}	volume of the sample in the ohmic cell (m^3)

swelling, the volume expansion of the starch granules results in a reduction in the distance between them; consequently, the quantity of unbound water decreases, leading to a reduction in the area for motion of the charged particles. When gelatinisation is completed and while the temperature continues to rise, the granules break down and leach amylose, increasing the amount of free water and causing the electrical conductivity to rise again. On the contrary, [Chaiwanichsiri et al. \(2001\)](#) observed an increase in electrical conductivity during starch gelatinisation. This was explained by the fact that they used pure water, unlike the previous authors. For this reason, the ions contained in the starch granules were released when the granules were disrupted after swelling, resulting in a significant increase in the electrical conductivity of the aqueous solution containing the starch. The background ion concentration after ion release had a stronger impact than that of the decrease in the unbound water content, increasing electrical conductivity instead of decreasing it.

Some modelling studies have been carried out on OH of solid food ([Icier and Ilicali, 2005a, 2005b; Marra, 2014; Marra et al., 2009; Shim et al., 2010](#)). However, to the authors' knowledge, modelling bread baking by OH has never been studied. Most of the above-mentioned studies showed that OH is not strictly isotropic, and that some cold points may appear as shown by [Marcotte \(1999\)](#). The hottest spot was located at the centre, while [Ito et al. \(2014\)](#) showed that the "corners" between the electrode and the cell wall may exhibit cold points.

The objective of this work was twofold: first, to study the behaviour of electrical conductivity in bread dough with different parameters (temperature, porosity, salt content). Second, to use a numerical simulation to predict the temperatures and understand the physical phenomena better, in such a way that it could be used for the sizing and, later, the development of an ohmic oven.

2. Materials and methods

2.1. Ohmic heating system

An ohmic cell was designed to measure the electrical conductivity of yeasted and non-yeasted bread dough. The experimental device consisted of a power supply (Rototransfo Dereix SA Paris R212, 0–220 V), two multimeters (AOIP MN 5128 as an ammeter and Fluke 45 as a voltmeter), a data logger (AOIP DATALOG 20) with an acquisition frequency of 0.15 Hz, and a computer. Two types of cell were made of a polypropylene cylindrical container, with an internal diameter of 29 mm and an external diameter of 32 mm.

The length of the cell was 98 mm for the first type and 61 mm for the second type. The electrodes were made of 2-mm-thick titanium, with a diameter of 28 mm, maintained in two polyoxymethylene caps of 20-mm thickness (10 mm inside the cell, 10 mm outside), allowing a gap between the electrodes of 78.7 mm (long cell) and 41.7 mm (short cell). Holes were made in both ohmic cells to adapt thermocouples (type K, insulated with a Teflon coating). The long cell had three holes, one at the centre and two at each side, 5 mm and 8 mm from the electrodes respectively. The short one had only one hole at the centre. The cells were put in a vertical position during the experiments. The ohmic cells and device are shown in [Fig. 1](#).

2.2. Sample preparation

The recipe used for the reference dough is given in [Table 1](#). Yeast was removed for the non-yeasted dough recipe. The impact of salt content on electrical conductivity was studied using non-yeasted dough. These samples were prepared with different salt contents (on dry basis): the reference dough (2.66%, following the recipe [Table 1](#)), double the reference salt weight (5.30%), 1.5 times (3.98%), 0.5 times (1.33%), and no salt. The dough was kneaded in a spiral mixer (VMI SPI 10, Montaigu, FRANCE) for 4 min at 50 rpm (spiral) and 6 rpm (bowl), and 5 min at 120 rpm (spiral) and 10 rpm (bowl). It was left for 15 min to rest, and then placed in the 78.7-mm cell. Contact was made with both electrodes, and the electrodes were immobilised in a stand to prevent volume change during heating. The electrical conductivity was measured immediately.

The impact of porosity on electrical conductivity was studied with yeasted dough. Five short cells, as described previously, were used. Because of the low electrical conductivity of the yeasted dough, it was necessary to use the shorter cell to obtain approximately the same heating rate with the same voltage as with the non-yeasted dough. Five different samples of yeasted dough were weighed and placed in the cells. The first one occupied the cell fully (contact with both electrodes) and was used as t_0 (no fermentation). The other samples were weighed in a decreasing order for an increasing fermentation time. The porosity was calculated using the following equation:

$$\varepsilon = 100 \times \left(1 - \frac{m_d}{V_{cell} \times \rho_0} \right), \quad (1)$$

with ε the porosity of the dough, m_d the weight of the dough sample, V_{cell} the volume of the cell in which the dough was contained, and ρ_0 the density of the degassed dough. The density of the

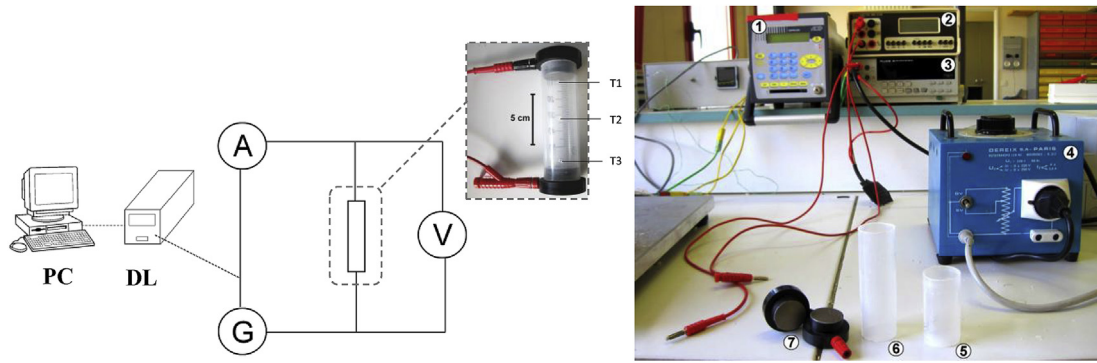


Fig. 1. Left: schematic view of the configuration. (PC) computer, (DL) data logger, (A) ammeter, (G) autotransformer, (V) voltmeter, (T) thermocouple. Right: OH device. (1) data logger, (2) ammeter, (3) voltmeter, (4) autotransformer, (5) short cell, (6) long cell, (7) electrodes.

Table 1
Sandwich bread recipe.

Ingredient	Origin	% (g/100 g of dough)
Wheat flour T65	Girardeau, Boussay, FRANCE	58.7
Water	Tap water	32.9
Sugar	Béghin Say, Tereos, FRANCE	2.9
Rapeseed oil	Rapsöl, Transgourmet, FRANCE	2.4
Salt	Cérébros, Esco France s.a.s, FRANCE	1.1
Skimmed milk powder	Délisse, FRANCE	0.9
Dehydrated yeast	Lesaffre, FRANCE	0.8
Purple IBIS dough improver	Lesaffre, FRANCE	0.3

degassed dough was calculated following a mixture model given in Eq. (2), using the density and the proportion of each ingredient of the dough (see Table 2):

$$\rho_0 = (X\rho)_{flour} + (X\rho)_{water} + (X\rho)_{yeast} + (X\rho)_{oil} + (X\rho)_{sugar} + (X\rho)_{salt} + (X\rho)_{milk} + (X\rho)_{improver}. \quad (2)$$

The cells were installed in a vertical position for fermentation. A mark was made 20 mm below the top of the cells (corresponding to the width of the electrodes and the inside caps) in order to achieve perfect contact between the dough and the electrodes when the dough reached the mark after fermentation. The cells were put in a proofing cabinet (Panimatic P1DB) at 27 °C and 85% RH, and the samples were removed when the dough reached the mark corresponding to the expected dough volume. For each expansion ratio of the dough, a sample was taken out of the fermentation cabinet, the caps (with electrodes) were inserted in the cell and the electrical conductivity was analysed immediately.

2.3. Thermophysical properties of the non-yeasted dough

The thermophysical properties of the non-yeasted dough were measured in order to implement these data in the numerical

model. The electrical conductivity was measured using the device presented previously. An AC voltage of 50 V and 50 Hz was applied to the sample. All data were acquired by the data logger: voltage, current and temperature evolution as a function of time. The electrical conductivity was calculated using the following equation:

$$\sigma = \frac{L \times I}{A \times V}, \quad (3)$$

where σ is the electrical conductivity in S/m, L the distance between electrodes in m, A the electrode area in m^2 , I the current in A, and V the voltage in V. The experimental data were implemented in the model (linear interpolation between the points).

The density of the non-yeasted dough was measured using the densimetric method first developed by Baker and Mize (1946). A 500-ml beaker was filled with oil (density: 916 kg m^{-3}) and placed on a scale. A holder was maintained in the oil, and the tare was set. The dough was weighed on the scale and then immersed in the oil; its apparent density was calculated using the following equation:

$$\rho_{app} = \frac{m_d \times \rho_{oil}}{m_i}, \quad (4)$$

with m_d the mass of dough, ρ_{oil} the density of the oil, and m_i the

Table 2
Density of each ingredient of the dough.

Ingredient	Density (kg m^{-3})	Reference
Flour	1450.0	Measured with a gas pycnometer (Fofonoff and Millard, 1983)
Water	998.2 (at 20 °C)	United States Department of Agriculture (USDA)
Yeast	1405.7	(Molle, 1985)
Rapeseed oil	916.0	Hazardous Substances Data Bank
Sugar	1592.1	Hazardous Substances Data Bank
Salt	2153.9	(Crossley, 1966)
Powder milk	1390.0	Assumed equal to flour
Improver	1450.0	

mass of dough when weighing immersed in the oil. The density of non-yeasted dough ρ_{app} differs from that of degassed dough ρ_0 in Eq. (2) due to the fact that air is introduced into the dough during kneading, while ρ_0 represents the density of perfectly degassed dough.

The thermal conductivity of the non-yeasted dough was measured based on the method proposed by Jury et al. (2007), using a line-heat source probe.

The heat capacity was measured by microcalorimetry, with a micro DSC III Setaram (SETARAM, Caluire – FRANCE). A heating rate of 1.2 °C/min was used from 20 to 115 °C.

2.4. Model development

The thermophysical properties determined previously were implemented in the numerical model. A linear interpolation was made between the experimental data points. Numerical modelling was carried out using Comsol Multiphysics® 5.1. The governing equation used was Laplace's, which describes the distribution of electrical potential within a food; and the heat transfer equation, using a source term involving the displacement of electrical potential. The electrical potential distribution within the dough was computed using the following Laplace equation:

$$\nabla \cdot \sigma \nabla V = 0. \tag{5}$$

The electrical potential distribution and electrical conduction generate a certain density of power in the product, described by the generation term in the following equation:

$$Q_{GEN} = \sigma |\nabla V|^2, \tag{6}$$

where $|\nabla V|$ represents the modulus of the gradient of electrical potential. The heat transfer occurring is described by the unsteady state heat equation by conduction, to which is added the source term (6):

$$\rho_{app} C_p \frac{\partial T}{\partial t} = \nabla k \nabla T + Q_{GEN}, \tag{7}$$

where T is the temperature within the product, t is the process time, k is the thermal conductivity, C_p is the heat capacity, and Q_{GEN} the ohmic power source (6). Heat losses were applied in the model: (i) by natural convection, assimilating the vertical cylinder to a vertical plate according to Churchill and Chu correlation (Bergman et al., 2011), and (ii) by radiation. The assumptions were made that: (i) most heat losses occurred between the cell wall in contact with the product and the environment, so the heat losses were only applied on this surface during numerical modelling; (ii) ρ_{app} was constant over the temperature range; and (iii) the porosity was uniform in size and distribution throughout the product.

A mesh independence study was carried out; the resulting mesh was constituted by 7014 elements (triangles) with 28950 degrees of freedom.

Experimental and predicted results were compared by calculating the average relative errors E_r , using the following equation:

$$E_r = \frac{100}{n} \sum_{i=1}^n \frac{\sqrt{(y_{Ei} - y_{Pi})^2}}{y_{Pi}}, \tag{8}$$

with n the number of values, y_{Ei} the experimental values and y_{Pi} the predicted values.

3. Results and discussion

3.1. Electrical conductivity of non-yeasted dough

The electrical conductivity of the dough was determined using Eq. (3); its evolution with the temperature at the centre of the dough is shown in Fig. 2. The error bars are represented every minute only, in order to get a clear view. The curve exhibits a three-stage pattern. The first stage is linear ($R^2 > 0.999$ for each one of the replications) until around 60 °C. During the second stage, the rate of electrical conductivity increase slows down (when reaching about 0.80 S m⁻¹), and the electrical conductivity starts to decrease slightly. This second stage can almost be assimilated to a plateau. Around 76 °C, the electrical conductivity starts to increase again, reaching a linear increase rate after about 80 °C ($R^2 > 0.99$). The temperature at which the linear evolution of electrical conductivity stops corresponds to the beginning of starch gelatinisation. This pattern is consistent with that observed by Li et al. (2004) with starch solutions. The area for the motion of electrolytes starts to decrease at the onset temperature as the swelling of starch begins, until the endset temperature at which all starch is gelatinised, and then electrical conductivity starts to rise again linearly. However, as mentioned by Li et al. (2004), the slopes ($d\sigma/dT$) are different before and after starch gelatinisation. This fact means that there is a modification in the dependence of electrical conductivity on temperature and suggests a change in the product, and therefore in the displacement of the electrical current. The authors suggested that this was due to the viscosity of the starch solution, higher after starch gelatinisation than before, which in our case could be assimilated to the dough/crumb transition.

3.2. Impact of porosity on electrical conductivity

The electrical conductivity of yeasted dough at different porosities is shown in Fig. 3. It can be observed that the higher the porosity - and therefore the longer the fermentation time, the lower the electrical conductivity. Yet, the shape of the curves does not change; the slopes are different but the gelatinisation stages remain almost identical. Onset temperatures are in the same range (60.2 ± 1.0 °C), as well as endset temperatures (76.6 ± 0.9 °C). The slopes before and after gelatinisation are almost identical for the non-yeasted dough and the yeasted dough at 10.75% porosity (0.64 ± 0.03 S m⁻¹ °C⁻¹ and 0.61 ± 0.03 S m⁻¹ °C⁻¹ respectively), because the 10.75% dough only underwent a very short fermentation (between ingredient mixing and testing). For all porosities, $d\sigma/dT$

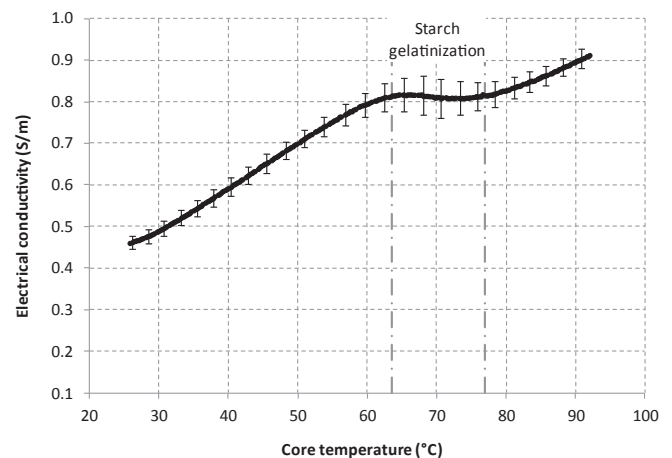


Fig. 2. Electrical conductivity of non-yeasted dough vs. temperature.

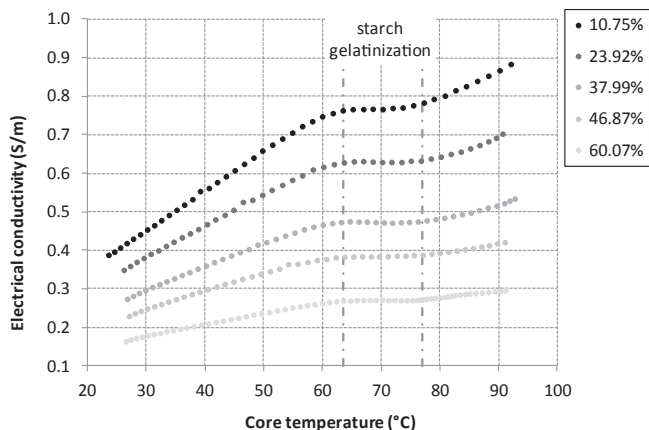


Fig. 3. Electrical conductivity of yeasted dough according to its porosity vs. temperature.

dT after starch gelatinisation is lower than before gelatinisation, as mentioned above. In each case, there is a difference of 32–48% between the slopes before and after gelatinisation.

All slopes decrease with the increase in porosity (from 0.0109 to 0.0029 $S\ m^{-1}\ ^\circ C^{-1}$). This can be explained by the fact that the difference in porosity for the different samples comes from gas production (CO_2) by yeast during fermentation, which conducts electricity very poorly. Fig. 4 represents the evolution in the value of electrical conductivity at 25 °C (determined by regression on the linear part of the curves), which is usually the reference temperature for electrical conductivity comparisons, and 50 °C vs. dough porosity. It can be observed that the decrease in electrical conductivity with porosity is linear ($R^2 = 0.98$ at 25 °C, $R^2 = 0.99$ at 50 °C). This linearity in this range of porosity (10.8–60.1%) is interesting. As indicated in different works – for example, Palaniappan and Sastry (1991) – electrical conductivity can be calculated using the electrical conductivity at a reference temperature (here 25 °C) as follows:

$$\sigma(T) = \sigma_{25}[1 + m(T - 25)], \quad (9)$$

with m a constant. This relation applies only during the linear evolution of electrical conductivity with temperature, meaning in this case before or after starch gelatinisation. As the electrical conductivity at a given temperature is linearly correlated with the porosity of the dough (see Fig. 4), Eq. (9) can be written as a

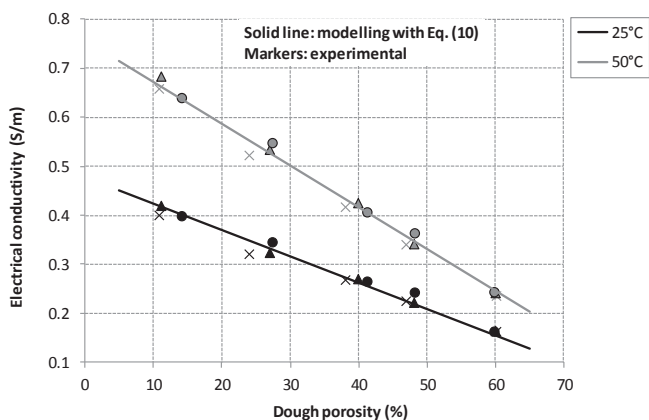


Fig. 4. Electrical conductivity at $T = 25\ ^\circ C$ and $50\ ^\circ C$ vs. porosity of yeasted dough. The three different symbols represent the replications.

function of porosity:

$$\sigma(\varepsilon, T) = (a_\varepsilon \varepsilon + b_\varepsilon)[1 + m_\varepsilon(T - 25)], \quad (10)$$

with a_ε and b_ε two constants. Their values for use in the equation before starch gelatinisation were obtained by minimising the sum of squared differences between the equation and the experimental data, and are given in Table 3. Eq. (10) was used for the linear regressions in Fig. 4.

3.3. Impact of salt content on electrical conductivity

The evolution of the electrical conductivity of non-yeasted dough as a function of temperature for selected salt contents on a dry basis (0.00%, 1.33%, 2.66%, 3.98%, and 5.30%) is shown in Fig. 5. As expected, the salt content has a clear impact on the electrical conductivity of the dough: the initial values are higher, as well as the rates of increase with respect to temperature and salt content. The dough without salt has a very low electrical conductivity, showing the importance of salt. To compare electrical conductivities at the same temperature, Fig. 6 shows the values at 25 and 50 °C vs. salt content. Electrical conductivity increases linearly with salt content ($R^2 = 0.991$ at 25 °C and $R^2 = 0.989$ at 50 °C) in our range of work (0.00–5.30% db) as expected. When placed in solution (here, free water), NaCl dissolves into Na^+ and Cl^- ions, improving the electrical conductive abilities of the sample. This shows the importance of the formulation in the management of the heating process, and how the heating profile of the product could be modified by slightly adjusting the salt content of the dough. As for porosity, and using Eq. (9), the calculation of electrical conductivity can be written as follows:

$$\sigma(S, T) = (a_S S + b_S)[1 + m_S(T - 25)], \quad (11)$$

with a_S and b_S two constants, and S the salt content in % db. Their values for use in the equation before starch gelatinisation were obtained by the same method as previously, and are given in Table 3. Eq. (11) was used for the linear regressions in Fig. 6.

3.4. Numerical modelling

3.4.1. Thermophysical properties of non-yeasted dough

The electrical conductivity of non-yeasted dough was directly integrated into the model (linear interpolation between the points) using data from Fig. 2.

Its density was measured as $1195.40 \pm 2.95\ kg\ m^{-3}$.

In the range of the current study (from 20 to 100 °C), the results of thermal conductivity according to the temperature of the dough could be modelled using the following equation ($R^2 = 0.993$):

$$k(T) = 5.22 \times 10^{-2} \ln T + 2.37 \times 10^{-1}. \quad (12)$$

The results correspond to those obtained by Zúñiga and Le-Bail (2009). They found $0.42\ W\ m^{-1}\ K^{-1}$ for a gas-free dough at 35 °C,

Table 3

Values of constants for modelling electrical conductivity as a function of the porosity, salt content and temperature of the dough.

Constant	Value	Unit
a_ε	-0.0054	$S\ m^{-1}$
b_ε	0.4786	$S\ m^{-1}$
m_ε	0.0232	$^\circ C^{-1}$
a_S	0.1583	$S\ m^{-1}$
b_S	0.0881	$S\ m^{-1}$
m_S	0.0262	$^\circ C^{-1}$

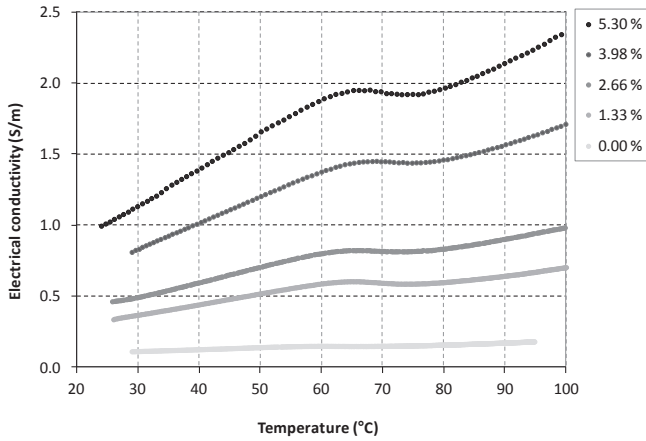


Fig. 5. Electrical conductivity of dough vs. core temperature as a function of salt content (dry basis).

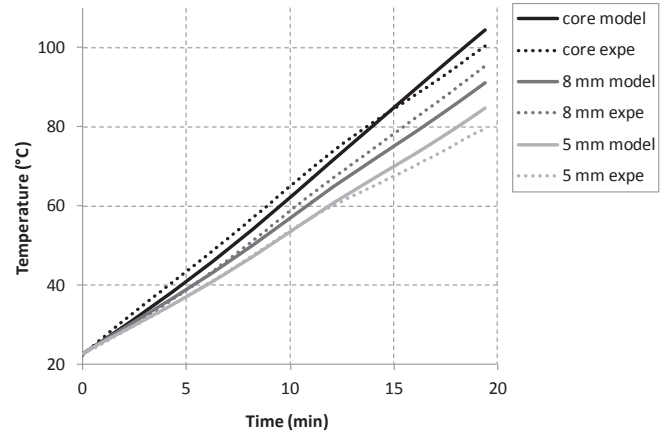


Fig. 8. Experimental measurements of temperatures at three locations in the product (centre, one side 8 mm from the electrode, the other side 5 mm from the electrode), and fitted modelled results with application of a corrective coefficient.

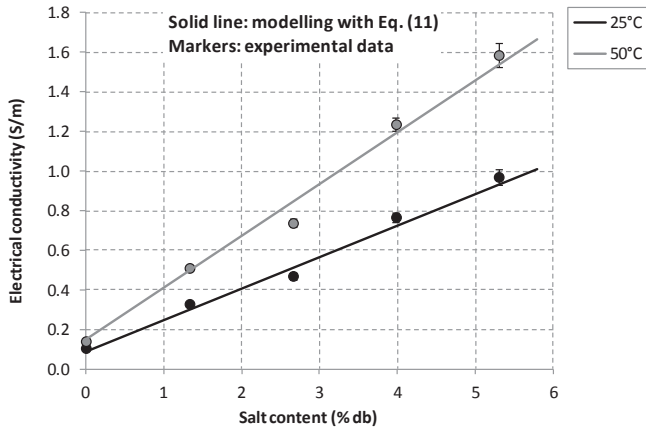


Fig. 6. Electrical conductivity of dough at T = 25 °C vs. salt content.

which is the exact same value as in this work, for a non-fermented dough (but not gas-free).

The data of heat capacity vs. temperature were directly integrated into the model, with a linear interpolation between the points and a linear extrapolation outside of the temperature analysis range. Both thermal conductivity and heat capacity vs. temperature are represented in Fig. 7; the error bars of heat capacity are represented every 2 °C for a clearer view, but the data were recorded every 0.008 °C.

3.4.2. Corrective coefficient

Numerical modelling showed a difference between the experimental and numerical results. In order to obtain a better correlation, a corrective coefficient was directly applied to the source term in (6), taking into account all energy losses other than heat losses by convection and radiation (electricity-to-heat conversion, inaccuracies in heat loss estimations), inaccuracies of data measurements, and uncertainties of cell geometry. The latter is usually defined by the cell constant in m^{-1} , theoretically obtained by the ratio of the gap between the electrodes and their area. The corrective coefficient was determined using an optimisation script under Matlab[®] 7.10.0 linked to Comsol Multiphysics[®]. The script was developed in our lab (Rouaud et al., 2011). Its principle was to minimise the sum of squared differences between experimental and numerical data for temperatures at three locations of the non-yeasted dough: the centre, one side at 8 mm from the electrode, and the other side at 5 mm from the second electrode. The value obtained was 0.8063, meaning that under perfect conditions, only 80.63% of the energy is used to produce heat. This value is in agreement with those obtained in previous works on energy efficiencies and electricity-to-heat conversion efficiencies. The energy efficiency of cooking meat by OH was found to be between 0.68 and 0.72 by de Halleux et al. (2005) and between 0.69 and 0.91 by Bozkurt and Icier (2010), while the electricity-to-heat conversion efficiency estimated by Ye et al. (2004) ranged from 0.78 to 0.85. The experimental measurements, as well as the fitted model results, are shown in Fig. 8.

Once experimental and numerical data were in fair agreement, the E_r (8) between experimental and numerical data were

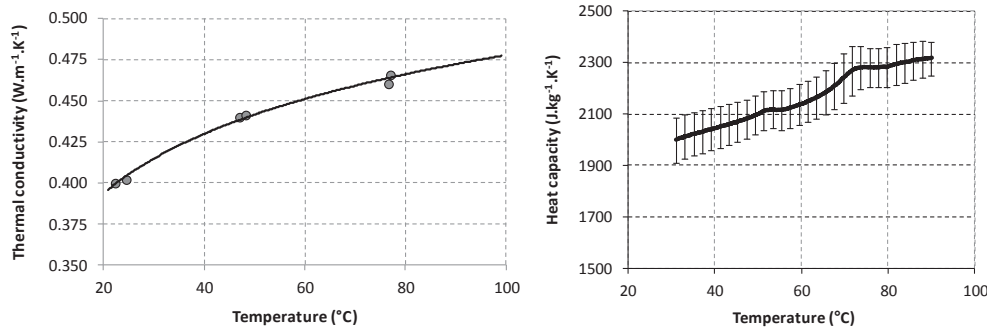


Fig. 7. Thermal conductivity (left) and heat capacity (right) of the dough vs. temperature.

Table 4
Average relative errors between experimental and numerical data for optimisation and validation steps of the model.

	Sample	E_r (%)
Determination of the coefficient	Reference, core	4.22
	Reference, 8 mm	2.76
	Reference, 5 mm	1.71
Validation	1.33% salt db.	2.27
	3.98% salt db.	3.80

calculated. The values are given in Table 4. The model with this corrective coefficient of 0.8063 was tested with two samples at different salt contents, i.e. 1.33 and 3.98% db, to verify that the coefficient was independent of electrical conductivity and to validate the model (Fig. 9). The experimental and numerical results were in good agreement too; the E_r (8) are given in Table 4. The results show that a simple model with no mass transfer can be used to predict the evolution of temperature during OH of bread dough with an acceptable precision.

3.4.3. Temperature profiles

The core temperature increased faster than the other two points (Fig. 8). For the experimental data, the average rate was $4.0\text{ }^\circ\text{C min}^{-1}$ at the core, 3.8 at 8 mm from the electrode and 2.9 at 5 mm . For the numerical data, the average rates were 4.2 , 3.5 and $3.2\text{ }^\circ\text{C min}^{-1}$, respectively. Heterogeneity in the temperatures has been observed by different authors, despite the theoretical homogeneous distribution of temperatures when using volumetric heating. The electrodes are responsible for this temperature gradient, as reported by Ito et al. (2014). The titanium electrodes do not heat up much due to their very low electrical resistivity, making them a cold spot. However, their thermal conductivity is high, which has the effect of easily dissipating heat from the product. Ito et al. (2014) observed that the coldest point in an ohmic cell was at the corner between the electrodes and the cell wall, because of the combination of the heat transfer to the outside from the wall and the heat dissipation from the electrode. This explains the results obtained in Fig. 8, showing that the closer to the electrode, the colder it is. To mitigate this phenomenon, Zell et al. (2011) found that using thinner electrodes could increase the temperature at the surface of electrodes, but the results did not show large differences between the final temperatures for various electrode thicknesses. Reducing the cell constant (ratio of the gap between electrodes and

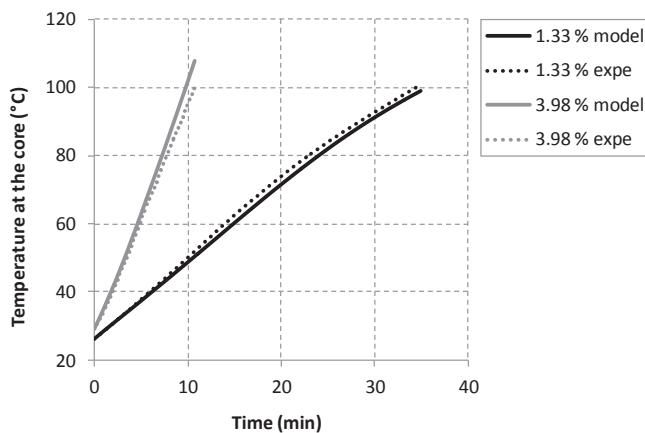


Fig. 9. Validation of the model with a corrective coefficient: experimental and modelled data for temperature measurements at the core of doughs at 1.33% and 3.98% salt content db.

their area) might also lead to better homogeneity in temperatures.

3.4.4. Heat losses

The parameters of the model were then used to simulate heating without heat losses. Fig. 10 shows the evolution of temperature at the core of the reference non-yeasted dough for numerical data with and without heat losses. Unlike the data from Fig. 8, the temperature of the model without heat losses followed an exponential trend, the heating rate increasing with time due to the dependence of electrical conductivity on temperature. This shows that the linear profile of temperature rise from experiments comes mainly from heat losses. Moreover, the final core temperature at $t = 19.4\text{ min}$ was $126\text{ }^\circ\text{C}$ for a perfectly insulated ohmic cell, against $104\text{ }^\circ\text{C}$ for the numerical results with heat losses. This shows the importance of good thermal insulation and the amount of energy that could be saved.

Fig. 11 shows the distribution of temperatures in the product, from the same modelled results. As suspected, the hottest spot in the ohmic cell was located at the core of the product, and the electrodes appeared as cold spots. Furthermore, the closer to them, the colder it was. Concerning the results with heat losses, the experimental observations of the underbaking of the dough (non gelatinisation of the starch) located close to the electrodes have confirmed the strong temperature gradient predicted by numerical simulations. Also, the surface of the product in contact with the wall of the cell was colder than the core, due to heat losses through the walls. These results are in agreement with those of Marra (2014) and Marra et al. (2009). On the contrary, for the results without heat losses, there was a homogeneity in temperatures on the x and y axes, but not in the z axis, because of the temperature gradient due to the electrodes acting as a heat sink. From numerical results, it appears that the difference between the core and electrode temperatures is higher with thermal insulation ($54.8\text{ }^\circ\text{C}$) than with heat losses ($44.3\text{ }^\circ\text{C}$), indicating that the thermal insulation of the wall is not the solution if we want to homogenize the temperature distribution along the z -axis.

4. Conclusion

In this work, the technical possibility of baking bread by OH was studied. It was shown that the electrical conductivity of a yeasted dough decreases linearly with its porosity. In addition, a slight change in the salt content of dough can greatly change its heating profile. This shows the importance of the formulation and fermentation of dough for the development of a baking method by

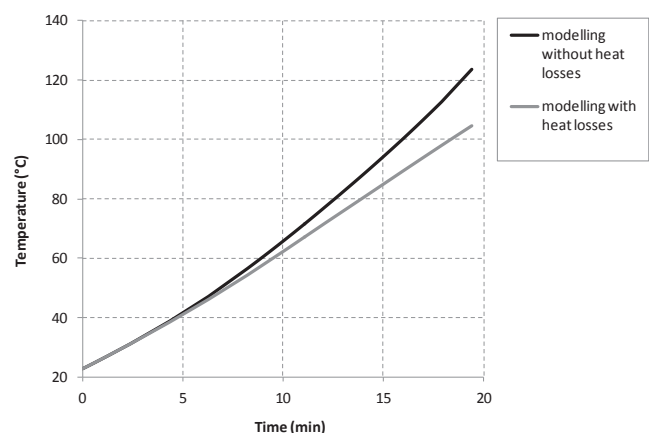


Fig. 10. Evolution of the core temperature for OH of reference dough, modelled with and without heat losses.

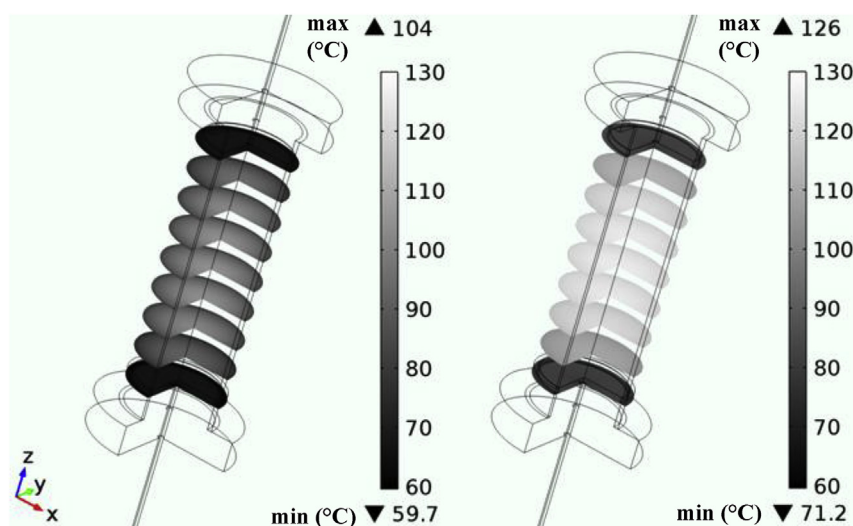


Fig. 11. Slice plot of non-yeasted reference dough after 1165 s of heating at 50 V, with (left) and without (right) heat losses.

OH. After calculating a corrective coefficient, numerical modelling performed very well and provided good correlation between the experimental and predicted results. The results show the impact of heat losses during bread baking by OH using such a device, and the importance of thermal insulation and other technical improvements to minimise temperature gradients inside the product.

This work can be of interest for industrial purposes. It helped to understand the behaviour of the bread dough during OH, contrary to other studies which investigated the impact of OH on bread as a final product. Further investigations need to be done with different ohmic cell configurations in order to study the impact on temperature gradients. Also, the effect of this baking method on heat and mass (water) transfers will be studied on a bigger scale.

Acknowledgments

The authors would like to thank Anthony Ogé and Luc Guihard for their technical support.

References

- Baker, J.C., 1939. A method and apparatus for testing doughs. *Cereal Chem.* 16, 513–517.
- Baker, J.C., Mize, M.D., 1939a. Effect of temperature on dough properties. I. *Cereal Chem.* 16, 517–533.
- Baker, J.C., Mize, M.D., 1939b. Effect of temperature on dough properties. II. *Cereal Chem.* 16, 682–695.
- Baker, J.C., Mize, M.D., 1941. The origin of the gas cell in bread dough. *Cereal Chem.* 18, 19–34.
- Baker, J.C., Mize, M.D., 1946. Gas occlusion during dough mixing. *Cereal Chem.* 23, 39–51.
- Bergman, T.L., Lavine, A.S., Incropera, F.P., Dewitt, D.P., 2011. *Fundamentals of Heat and Mass Transfer*, seventh ed.
- Bozkurt, H., Icier, F., 2010. Exergetic performance analysis of ohmic cooking process. *J. Food Eng.* 100, 688–695.
- Chaiwanichsiri, S., Ohnishi, S., Suzuki, T., Takai, R., Miyawaki, O., 2001. Measurement of electrical conductivity, differential scanning calorimetry and viscosity of starch and flour suspensions during gelatinisation process. *J. Sci. Food Agric.* 81, 1586–1591.
- Crossley, E.L., 1966. Le lait sec. In: *Hygiène Du Lait*. World Health Organization, pp. 351–411.
- de Halleux, D., Piette, G., Buteau, M.-L., Dostie, M., 2005. Ohmic cooking of processed meats: energy evaluation and food safety considerations. *Can. Biosyst. Eng.* 47, 41–47.
- Derde, L.J., Gomand, S.V., Courtin, C.M., Delcour, J.A., 2014. Moisture distribution during conventional or electrical resistance oven baking of bread dough and subsequent storage. *J. Agric. Food Chem.* 62, 6445–6453.
- Fofonoff, N.P., Millard, R.C., 1983. Algorithms for Computation of Fundamental Properties of Seawater (UNESCO Technical papers in marine science).
- Hayman, D., Hosney, R.C., Faubion, J.M., 1998. Effect of pressure (crust formation) on bread crumb grain development. *Cereal Chem.* 75, 581–584.
- He, H., Hosney, R.C., 1991a. A critical look at the electric resistance oven. *Cereal Chem.* 68, 151–155.
- He, H., Hosney, R.C., 1991b. Gas retention in bread dough during baking. *Cereal Chem.* 68, 521–524.
- Hosney, R.C., 1986. Component interaction during heating and storage of baked products. In: *Blanshard, J.M.V., Frazier, P.J. (Eds.), Chemistry and Physics of Baking*. Royal Society of Chemistry (Great Britain). Food Chemistry Group, University of Nottingham, School of Agriculture, Sutton Bonington, pp. 216–226.
- Icier, F., Ilicali, C., 2005a. The use of tylose as a food analog in ohmic heating studies. *J. Food Eng.* 69, 67–77.
- Icier, F., Ilicali, C., 2005b. Temperature dependant electrical conductivities of fruit purees during ohmic heating. *Food Res. Int.* 38, 1135–1142.
- Ito, R., Fukuoka, M., Hamada-Sato, N., 2014. Innovative food processing technology using ohmic heating and aseptic packaging for meat. *Meat Sci.* 96, 675–681.
- Junge, R.C., Hosney, R.C., 1981. A mechanism by which shortenings and certain surfactants improve loaf volume in bread. *Cereal Chem.* 58, 408–412.
- Jury, V., Monteau, J.-Y., Comiti, J., Le-Bail, A., 2007. Determination and prediction of thermal conductivity of frozen part baked bread during thawing and baking. *Food Res. Int.* 40, 874–882.
- Luyts, A., Wilderjans, E., Van Haesendonck, I., Brijs, K., Courtin, C.M., Delcour, J.A., 2013. Relative importance of moisture migration and amylopectin retrogradation for pound cake crumb firming. *Food Chem.* 141, 3960–3966.
- Marcotte, M., 1999. *Ohmic Heating of Viscous Liquids*. McGill University, Sainte-Anne-de-Bellevue.
- Marra, F., 2014. Mathematical model of solid food pasteurization by ohmic heating: influence of process parameters. *Sci. World J.* 2014, 1–8.
- Marra, F., Zell, M., Lyng, J.G., Morgan, D.J., Cronin, D.A., 2009. Analysis of heat transfer during ohmic processing of a solid food. *J. Food Eng.* 91, 56–63.
- Martin, M.L., Zeleznak, K.J., Hosney, R.C., 1991. A mechanism of bread firming. I. Role of starch swelling. *Cereal Chem.* 68, 498–503.
- Molle, J.-F., 1985. Biocarburants. *Tech. l'Ingénieur A1770*, 20.
- Palaniappan, S., Sastry, S., 1991. Electrical conductivities of selected solid foods during Ohmic heating. *J. Food Process Eng.* 14, 221–236.
- Rouaud, O., Curet-Ploquin, S., Chevallier, S., 2011. Numerical Estimation of the Effective Moisture Diffusivity during Microwave Heating of Food. *Icef11*, Athens, Greece. May 22–28, 2011.
- Sakr, M., Liu, S., 2014. A comprehensive review on applications of ohmic heating (OH). *Renew. Sustain. Energy Rev.* 39, 262–269.
- Sarang, S., Sastry, S.K., Knipe, L., 2008. Electrical conductivity of fruits and meats during ohmic heating. *J. Food Eng.* 87, 351–356.
- Sastry, S.K., 1989. A model for continuous sterilization of particulate foods by ohmic heating. In: *Present. 5th Int. Cong. Eng. Food, Col. Ger.* May 28–June 03, 1989.
- Shelke, K., Faubion, J.M., Hosney, R.C., 1990. The dynamics of cake baking as studied by a combination of viscometry and electrical resistance oven heating. *Cereal Chem.* 67, 575–580.
- Shim, J., Hyun, S., Jun, S., 2010. Modeling of ohmic heating patterns of multiphase food products using computational fluid dynamics codes. *J. Food Eng.* 99, 136–141.
- Li, F., De Li, L., Te Li, Z., Tatsumi, E., 2004. Determination of starch gelatinization temperature by ohmic heating. *J. Food Eng.* 62, 113–120.

- Wang, W.-C., Sastry, S.K., 1997. Starch gelatinization in ohmic heating. *J. Food Eng.* 34, 225–242.
- Ye, X., Ruan, R., Chen, P., Doona, C., 2004. Simulation and verification of ohmic heating in static heater using MRI temperature mapping. *Leb. Wiss Technol. Food Sci. Technol.* 37, 49–58.
- Zell, M., Lyng, J.G., Morgan, D.J., Cronin, D.A., 2011. Minimising heat losses during batch ohmic heating of solid food. *Food Bioprod. Process* 89, 128–134.
- Zúñiga, R., Le-Bail, A., 2009. Assessment of thermal conductivity as a function of porosity in bread dough during proving. *Food Bioprod. Process* 87, 17–22.